

Virtual fluoroscopy during transbronchial biopsy for locating ground-glass nodules not visible on X-ray fluoroscopy

Toshiyuki Nakai¹, Takehiro Izumo², Yuji Matsumoto¹, Takaaki Tsuchida¹

¹Department of Endoscopy, Respiratory Endoscopy Division, National Cancer Center Hospital, Tsukiji, Chuo-ku, Tokyo, Japan; ²Department of Respiratory Medicine, Japanese Red Cross Medical Center, Hiroo, Shibuya-ku, Tokyo, Japan

Contributions: (I) Conception and design: T Izumo, T Nakai; (II) Administrative support: T Izumo, T Tsuchida; (III) Provision of study materials or patients: All authors; (IV) Collection and assembly of data: Y Matsumoto, T Nakai; (V) Data analysis and interpretation: T Izumo, T Nakai; (VI) Manuscript writing: All authors; (VII) Final approval of manuscript: All authors.

Correspondence to: Takehiro Izumo. Department of Respiratory Medicine, Japanese Red Cross Medical Center, 4-1-22 Hiroo, Shibuya-ku, Tokyo 150-8935, Japan. Email: drtake1118@gmail.com.

Background: Virtual fluoroscopy (VF) is a novel guided technique that provides ray summation images of target lesions similar to X-ray fluoroscopy. Endobronchial ultrasound with a guide sheath (EBUS-GS) is a useful modality for imaging ground-glass nodules (GGNs) but is not ideal for GGNs that cannot be detected on X-ray fluoroscopy. We evaluated whether the addition of VF to EBUS-GS improved the diagnostic yield.

Methods: Consecutive patients who had undergone diagnostic bronchoscopy for GGNs that were not detected on X-ray fluoroscopy between September 2012 and January 2016 were retrospectively enrolled. The patients were divided into two groups: a non-VF group [performed using conventional thin-section computed tomography (CT), X-ray fluoroscopy, EBUS-GS, and virtual bronchoscopy for reference], and a VF group (performed using additional VF to non-VF group). We then compared the diagnostic yields between the two groups and performed a multivariate analysis to identify factors associated with an increased diagnostic yield.

Results: A total of 74 patients (VF, 35 patients; non-VF, 39 patients) were enrolled and were included in the analysis. The diagnostic yield was significantly higher in the VF group (77.1%) than in the non-VF group (51.2%, $P=0.030$). There were no clinically significant complications in either group. In the multivariate analysis, a positive bronchus sign [odds ratio (ORs), 5.41; 95% confidence interval (CI), 1.36–21.40] and the use of VF (odds ratio, 3.68; 95% confidence interval, 1.16–11.60) were significantly associated with successful bronchoscopic diagnosis.

Conclusions: The addition of VF to EBUS-GS helped to identify GGNs that were not visible on X-ray fluoroscopy.

Keywords: Lung cancer; ground-glass nodule (GGN); bronchoscopy; virtual fluoroscopy (VF); virtual bronchoscopy (VB); radial endobronchial ultrasound with a guide sheath (EBUS-GS)

Submitted Apr 05, 2017. Accepted for publication Sep 24, 2017.

doi: 10.21037/jtd.2017.10.01

View this article at: <http://dx.doi.org/10.21037/jtd.2017.10.01>

Introduction

One consequence of the National Lung Screening Trial (NLST), which reported a 20% reduction in mortality after the introduction of low-dose helical computed tomography (CT) screening, has been an increase in the detection of

patients with pulmonary ground-glass nodules (GGNs) (1,2). GGNs are clinically common and are worrisome because they can be found in not only a wide variety of benign conditions, but also early-stage lung cancer (3,4). Before GGNs can be treated appropriately, a pathological diagnosis is necessary. Multiple modalities to establish

a tissue diagnosis for GGNs are available, including surgical biopsy, CT-guided needle biopsy (CTNB), and bronchoscopy. Although surgical biopsy and CTNB have high diagnostic yields for GGNs regardless of their visibility on X-ray fluoroscopy (5,6), these procedures are associated with a risk of unnecessary excision for surgical biopsies (9–23%) (7–9) and a risk of tension pneumothorax (0.10%), tumor seeding (0.061%), and air embolism (0.061%) for CTNB (10).

Bronchoscopy is a safe and effective diagnostic method for peripheral pulmonary lesions (PPLs), and the most frequent complication, pneumothorax, occurs in only 1.5% of procedures (11). Recent reports of bronchoscopy using endobronchial ultrasound with a guide sheath (EBUS-GS) and virtual bronchoscopy (VB) for the diagnosis of GGNs were based on data involving GGNs that were visible on X-ray fluoroscopy (12–14). However, GGNs are often not visible on X-ray fluoroscopy even if the C-arm gantry angle is adjusted, potentially influencing the clinical diagnostic yield of bronchoscopy (13,15).

Virtual fluoroscopy (VF) is a novel navigation system for bronchoscopy that can be used in combination with EBUS-GS and VB. VF can clearly show the location of target lesions in ray summation images, similar to X-ray fluoroscopy. VF imaging can thus be used as a reference for biopsy sites during bronchoscopy regardless of the visibility on GGNs on real-time X-ray fluoroscopy. The use of VF for bronchoscopy has been previously described (16), and unlike other guiding techniques, VF images can be easily and quickly constructed from multi-slice CT volume data and workstations without additional cost. The present study evaluated the diagnostic utility of VF in addition to EBUS-GS with VB for GGNs that were not visible on X-ray fluoroscopy.

Methods

Patients

Consecutive patients who underwent a diagnostic bronchoscopy for GGNs in the Respiratory Endoscopy Division of the National Cancer Center Japan between September 2012 and February 2016 were retrospectively identified. Among them, cases with GGNs that were not visible on X-ray fluoroscopy were enrolled. Cases with GGNs visible on chest X-ray images obtained prior to bronchoscopy were excluded. Based on the additional use of VF for intraoperative referencing, the patients were

divided into two groups: a non-VF group (performed using conventional thin-section CT (TSCT), X-ray fluoroscopy, EBUS-GS, and VB for reference), and a VF group (performed using additional VF to non-VF group). GGNs were defined as rounded areas with a slight, homogenous increase in density and preservation of the underlying vessels and bronchi (17) and were classified as nonsolid nodules, which were lesions with no solid components, or as part-solid nodules, which contained heterogeneous attenuation with some solid components. Diagnostic yield was defined as the percentage of cases with a positive diagnosis. This study was conducted retrospectively and was approved by the National Cancer Center Institutional Review Board (No. 2012-278). Written informed consent was obtained from all the patients prior to bronchoscopy.

EBUS-GS equipment and GGN procedures

All the patients were evaluated using TSCT scanning (≤ 1 mm slice thickness) with an 80-detector row CT (Aquilion PRIME; TOSHIBA, Tokyo, Japan) within 4 weeks of bronchoscopy. The images were displayed with a lung window setting (center, -600 Hounsfield units; width, $1,500$ Hounsfield units). VB (Ziostation2[®], Ziosoft Ltd., Tokyo, Japan) was prepared from chest CT data for all the patients prior to bronchoscopy. All the procedures were performed through the oral route using a fiberoptic bronchoscope (BF-P260F or BF-1T260; Olympus, Tokyo, Japan) in combination with an R-EBUS probe (UM-S20-17S or UM-S20-20S; Olympus, Tokyo, Japan) and a guide sheath kit (K-201 or K-203; Olympus, Tokyo, Japan) under local anesthesia with conscious sedation. Upon reaching the target bronchus, the R-EBUS probe, which was covered with the guide sheath, was inserted through the working channel of the bronchoscope and adjusted under real-time X-ray fluoroscopic guidance (VersiFlex VISTA[®], Hitachi, Japan) until an EBUS image of the GGN was obtained.

EBUS images were classified as “within”, “adjacent to”, or “not visible”. The probe, covered with the guide sheath, was adjusted as much as possible (18,19), and if an EBUS image could not be visualized, as in the case of a solid lesion, the probe was manipulated under X-ray fluoroscopic guidance until a whitish acoustic shadow, i.e., a blizzard sign or mixed blizzard sign, was visualized (20,21). After the lesions were detected by the R-EBUS, samples for pathological and cytological evaluation were obtained through the guide sheath using forceps and a brush. VF was additionally used as a reference for determining the lesion

location when the operator deemed that detecting the lesion was difficult (e.g., when obtaining the EBUS images seemed difficult or when the biopsy site was unclear on real-time fluoroscopic imaging after the removal of the R-EBUS probe). After each sampling, the devices were rinsed with 5 mL of normal saline, and the fluid samples were sent for microbiological analysis and cytological examinations (22).

VF

VF was used as a means of navigation in addition to EBUS-GS and VB. Multidetector CT images with a slice thickness of 0.5 or 1.0 mm were transferred to a workstation (Ziostation2[®]; Ziosoft Ltd., Tokyo, Japan) for constructing VB. The VB was constructed using a previously reported method (23). VF images were then constructed from the volume data obtained from multidetector CT imaging using the Ziostation2[®]; the target lesion was extracted, and a trace line was drawn to create a VB from the trachea to the target lesion along the connecting bronchus on a ray summation image similar to X-ray fluoroscopy (16). The density of the target GGN was adjusted so that it was visible on the ray summation image using a window level of 350–1,000 Hounsfield units and a window width of 3,000–3,600 Hounsfield units. The images were then displayed at any angle using 3-dimensional VF imaging. The construction of the VF images was completed by connecting the background, which was reconstructed on the ray summation image, and the target lesion with the trace line. Finally, the optimal working angle for the bronchoscopy was determined by rotating the VF image. The construction of the VF image during VB processing required approximately 1 additional minute.

Diagnostic criteria for bronchoscopy samples

Histological findings of malignancy or cytological class IV/V findings were considered diagnostic. Samples with specific benign findings (e.g., necrotizing epithelioid granuloma, inflammation) or positive microbiological cultures were also considered diagnostic. Lesions with no significant pathologic or microbiological findings and that had decreased in size at a 6-month CT follow-up examination were reported as inflammation. Patients who could not be diagnosed by bronchoscopy or with lesions that did not decrease in size after a CT follow-up examination were diagnosed by surgical biopsy.

Assessment

To evaluate the utility of the addition of VF to the conventional method, the diagnostic yields of the non-VF and VF groups were compared. The Fischer exact test was used for categorical data and the Mann-Whitney U test was used for numerical data to assess the significance of differences in patient characteristics and bronchoscopy results observed between the non-VF and VF groups. Patient age, sex, lesion diameter, location (right upper lobe/left upper segment, right middle lobe/left lingula, or bilateral lower lobes), distribution (outer or inner), consolidation/tumor ratio (C/T ratio) on CT ($\leq 25\%$ or $>25\%$), presence of a bronchus sign on TSCT (positive or negative), and type of guide sheath kit (small or large) were recorded. Lesion diameter was recorded as the longest diameter on axial TSCT images. Lesion distribution was determined as previously reported and was designated as “central” if it was within the inner or middle third ellipse or “peripheral” if it was within the outer third ellipse (23). The C/T ratio was defined as the maximum diameter of the consolidation component relative to the maximum lesion diameter. A bronchus sign on TSCT was regarded as the presence of a bronchus leading directly to or contained within a target lesion (24,25). The bronchoscopy results included the procedure time, the bronchial generation of bronchoscope inserted, EBUS images, and the diagnostic yield. The procedure time was the interval between the insertion and removal of the bronchoscope through the vocal cords.

Factors affecting the diagnostic yield were analyzed using the Fischer exact test. Variables with $P < 0.20$ were included in a multivariate logistic regression model, and the odds ratio (OR) and 95% confidence interval (CI) were calculated. Descriptive statistics were reported as the frequency or percentage and the median \pm standard deviation. All the statistical tests were two-sided; $P < 0.05$ was considered to indicate statistical significance. All the statistical analyses were performed using EZR (Saitama Medical Center, Jichi Medical University, Saitama Japan), which is a graphical user interface for R (The R Foundation for Statistical Computing, Vienna, Austria) (26).

Results

A total of 74 patients were enrolled and analyzed. A summary of their baseline characteristics is shown in *Table 1*;

Table 1 Baseline characteristics of patients with GGNs that is not visible on X-ray fluoroscopy (n=74)

Variables	All (n=74)	Non-VF group (n=39)	VF group (n=35)	P value
Age (mean ± standard deviation) (years)	66.7±7.8	66.9±7.4	66.5±8.3	0.820
Sex, n (%)				0.642
Male	37 (50.0)	21 (53.8)	16 (45.7)	
Female	37 (50.0)	18 (46.2)	19 (54.3)	
Diameter of the lesion (mean ± standard deviation) (mm)	18.80±5.60	19.60±5.80	17.90±5.30	0.166
Location of the lesion, n (%)				0.857
Right upper lobe/left upper segment	35 (47.3)	18 (46.2)	17 (48.6)	
Right middle/left lingula	11 (14.9)	5 (12.8)	6 (17.1)	
Right lower/left lower	28 (37.8)	16 (41.0)	12 (34.3)	
Distribution of the lesion, n (%)				1.000
Outer area	59 (79.7)	31 (79.5)	28 (80.0)	
Inner area	15 (20.3)	8 (20.5)	7 (20.0)	
C/T ratio, n (%)				1.000
≤25	17 (23.0)	9 (23.1)	8 (22.9)	
>25	57 (77.0)	30 (76.9)	27 (77.1)	
Bronchus sign, n (%)				0.148
Positive	60 (81.1)	32 (82.1)	28 (80.0)	
Negative	14 (18.9)	7 (17.9)	7 (20.0)	
Guide sheath kit type, n (%)				0.790
K-203, large	55 (74.3)	28 (71.8)	27 (77.1)	
K-201, small	19 (25.7)	11 (28.2)	8 (22.9)	

GGNs, ground-glass nodules; VF, virtual fluoroscopy; C/T, consolidation-to-tumor.

no significant differences were seen between the non-VF and VF groups. The EBUS-GS and VB results are shown in *Table 2*. The overall GGN diagnostic yield was 63.5% (47/74), and all 27 patients who were not diagnosed by bronchoscopy were subsequently diagnosed by surgery. No significant differences in the mean procedure time, bronchial generation of bronchoscope inserted, or visualization of GGNs using EBUS were seen between the non-VF and VF groups ($P=0.4$, $P=0.34$, and $P=0.22$, respectively), but the diagnostic yield was significantly higher in the VF group (77.1%) than in the non-VF group (51.2%, $P=0.030$). Details of the final diagnoses in both groups are shown in *Table 3*. Two patients (2.7%) had complications; one patient in the VF group had mild disinhibition, and one patient in the non-VF group had a pneumothorax that did not require chest tube drainage. No

significant complications were observed.

A multivariate analysis (*Table 4*) found that both a positive bronchus sign (OR, 5.41; 95% CI, 1.36–21.40; $P=0.016$) and the use of VF (OR, 3.68; 95% CI, 1.16–11.6; $P=0.027$) had a significant effect on the diagnostic yield.

Representative patient results are shown in *Figure 1*. A 62-year-old man was diagnosed using TSCT as having a part-solid GGN measuring 16.1 mm in diameter and located in the right S9. The lesion was undetectable on both chest X-ray and X-ray fluoroscopy images. Prior to bronchoscopy, both VB and VF were constructed. We approached the target lesion through a preplanned bronchial route generated by the VB. The guide sheath and EBUS probe were inserted into the B9ai bronchus and were manipulated under real-time fluoroscopy with reference to the VF findings for guidance. The EBUS image showed a

Table 2 The results of bronchoscopy for GGNs (n=74)

Variables	non-VF group (n=39)	VF group (n=35)	P value
Procedure time (mean ± standard deviation) (min)	23.3±9.0	23.1±5.6	0.400
Bronchial generation of bronchoscope inserted (mean ± standard deviation)	5.3±1.0	5.1±1.3	0.340
EBUS images, n (%)			0.220
Within	22 (56.4)	26 (74.3)	
Adjacent to	7 (17.9)	5 (14.3)	
Invisible	10 (25.6)	4 (11.4)	
Diagnostic yield, n (%)	20 (51.2)	27 (77.1)	0.030

VF, virtual fluoroscopy; EBUS, endobronchial ultrasound; GGNs, ground-glass nodules.

Table 3 Final diagnosis of patients with GGNs

Final diagnosis	All GGNs
Adenocarcinoma	67
Adenocarcinoma in situ	3
Minimally invasive adenocarcinoma	2
Malignant lymphoma	1
Organizing pneumonia	1

GGNs, ground-glass nodules.

subtle but noticeable increase in the intensity and radius of the whitish acoustic shadow (i.e., blizzard sign). Using the guide sheath kit, the biopsy site was determined by referring to the VF. Histopathologic evaluation of the biopsy revealed an adenocarcinoma.

Discussion

To our knowledge, this is the first report on the diagnostic utility of combining VF, EBUS-GS, and VB for the diagnosis of lung lesions. The frequency of GGN detection has been increasing, and selecting a diagnostic modality can become a clinical problem for physicians (27,28). Several publications have evaluated the diagnostic utility of EBUS-GS for GGNs (12-14) that were or were not visible on X-ray fluoroscopy images. Previous studies have reported that the visibility of target lesions on X-ray fluoroscopy affects the diagnostic yield achieved by bronchoscopy (13,15). The yield of GGNs detection on fluoroscopy has been reported to be 42.6–45.0% (12-14). Most physicians recognize the clinical difficulties of diagnostic bronchoscopy for GGNs that cannot be visualized on X-ray fluoroscopy. The present

study showed that the addition of VF to EBUS-GS and VB for the diagnosis of GGNs not visible on X-ray fluoroscopy significantly improved the diagnostic yield.

VF is a novel guiding technique that can resolve some problems posed by GGNs that are not visible on X-ray fluoroscopy. Although confirming the location of a GGN on TSCT is easy, it can be difficult to locate the GGN on X-ray fluoroscopy images. However, VF can clearly visualize otherwise hazy GGNs with a trace line between the trachea and the target lesion on ray summation images, similar to X-ray fluoroscopy. VF can also show the position of a GGN in relation to the surrounding anatomical structures in one image at any angle. Thus, the best working angle for approaching a target lesion during bronchoscopy can be determined by referring to the VF findings prior to the procedure, and VF can be used as an intraoperative reference for determining the lesion location and for forceps guidance (*Figure 2*). The usefulness of VF for transhepatic biliary drainage has also been recently reported; thus, VF is likely to be useful in various fluoroscopic procedures, and its application is not limited to bronchoscopy.

When a peripheral lesion is approached through a transbronchial route, its location is usually confirmed by X-ray fluoroscopy and EBUS imaging. However, in the case of lesions that are not visible on X-ray fluoroscopy, confirmation depends entirely on the EBUS image. Therefore, it is important to visualize the target lesions using EBUS. Although GGNs often exhibit delicate changes on EBUS images (12-14,20,21), EBUS images could be obtained in 60 cases (81.1%) in the present study. This result suggests that confirming the location of GGNs using EBUS is a feasible method. In this study, there were no significant differences in the visualization of

Table 4 Logistic regression analysis of clinical factors on diagnostic yield of bronchoscopy with EBUS-GS and VB for not visible GGNs on X-ray fluoroscopy

Variables	Univariate analysis		Multivariate analysis	
	Diagnostic yield (%)	P value	OR (95 %CI)	P value
Age (years)		0.450	–	–
<70	28/47 (59.6)			
≥70	19/27 (70.4)			
Sex		0.330	–	–
Male	26/37 (70.3)			
Female	21/37 (56.8)			
Diameter of the lesion (mm)		0.130	3.39 (0.98–11.60)	0.052
≤20	27/48 (56.3)			
>20	20/26 (76.9)			
Location of the lesion		0.210	–	–
Right upper lobe/left upper segment	21/35 (60.0)			
Right middle/left lingula	5/11 (45.5)			
Lower	21/28 (75.0)			
Distribution		0.380	–	–
Outer area	39/59 (66.1)			
Inner area	8/15 (53.3)			
Consolidation/tumor ratio		0.150	2.60 (0.75–9.00)	0.130
≤25	8/17 (47.1)			
>25	39/57 (68.4)			
Bronchus sign		0.005	5.41 (1.36–21.40)	0.016
Positive	43/60 (71.7)			
Negative	4/14 (28.6)			
Using of VF		0.030	3.68 (1.16–11.60)	0.027
Yes	27/35 (77.1)			
No	20/39 (51.3)			
Guide sheath kit type		0.590	–	–
K-203, large	36/55 (65.5)			
K-201, small	11/19 (57.9)			

OR, odds ratio; CI, confidence interval; VF, virtual fluoroscopy; EBUS-GS, endobronchial ultrasound with a guide sheath; VB, virtual bronchoscopy; GGNs, ground glass nodules.

GGNs using EBUS between the non-VF and VF groups. However, the diagnostic yield was higher in the VF group than in the non-VF group. Why was there such a gap between the visualization rate of EBUS and the diagnostic

yield? Presumably, this gap arose because of the migration of the guide sheath from the target lesion as a result of coughing, positional discrepancy in selecting the biopsy site, or difficulty in redetecting the GGN on EBUS images

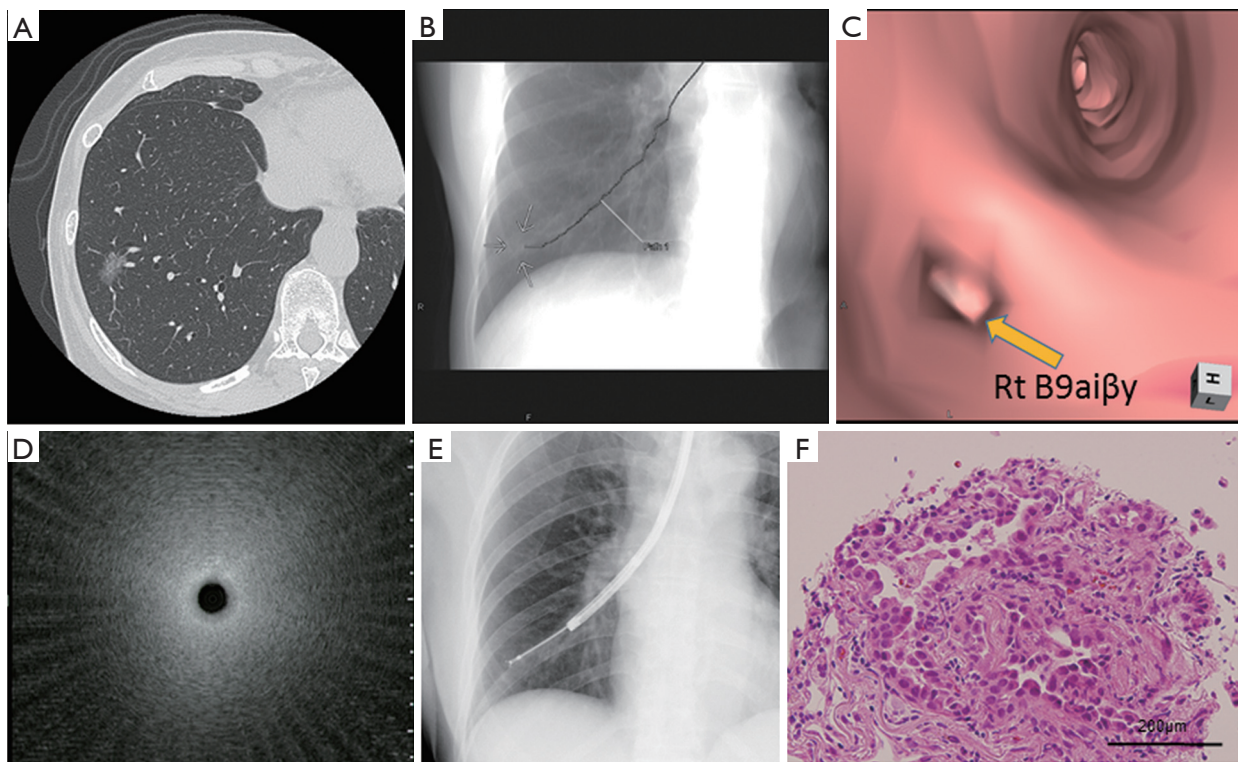


Figure 1 Computed tomography evaluation of a 62-year-old man with a part-solid ground-glass nodule (GGN) in the right lower lobe. CT revealed a lesion in the right S9a (A), but the lesion was not visible on X-ray images. The lesion was approached under guidance from virtual fluoroscopy (VF) findings showing the location of the lesion at the marked arrowhead and the trace line toward the target lesion on a ray summation image (B) as well as guidance from virtual bronchoscopy findings (C). Radial endobronchial ultrasound (EBUS) showed a blizzard sign (D). The biopsy site was chosen with reference to the VF and EBUS images (E). The biopsy specimen was diagnosed as an adenocarcinoma (hematoxylin-eosin staining, $\times 200$) (F). CT, computed tomography.

obtained after biopsy because of disturbances from bleeding. VF was useful in such situations as a reference for the lesion location and for forceps guidance during real-time fluoroscopic imaging after removal of the EBUS probe. The overall diagnostic yield (47/74, 63.5%) for EBUS-GS with VB was lower than previously reported (29), but the yield in the VF group (27/35, 77.1%) was comparable to that achieved in previous reports using bronchoscopy for GGNs that were visible on X-ray fluoroscopy images (12-14). It is important to construct VF and VB easily and quickly from volume data obtained from multi-slice CT and a workstation, with no additional cost. By combining these guiding techniques, the bronchoscope can be positioned as close as possible to the target lesion via a preplanned bronchus route constructed by VB. Next, the lesion can be detected on EBUS images, and final adjustments to the biopsy site can be performed based on real-time X-ray

fluoroscopy with VF guidance after the removal of the R-EBUS probe.

We found that the presence of a bronchus sign on TSCT was significantly associated with a successful diagnostic bronchoscopy. This finding is in line with several previous reports that a bronchus sign was a predictive factor for successful bronchoscopy for both GGNs and solid lesions (14). In the present study, univariate and multivariate analyses revealed that the presence or absence of a bronchus sign significantly affected the diagnostic yield (71.7% *vs.* 28.6%; OR, 3.68; 95% CI, 1.16–11.60). Bronchoscopy with EBUS-GS and VB appears to be the preferable diagnostic modality for GGNs with a positive bronchus sign. In the absence of the bronchus sign, transbronchial needle aspiration with a guide sheath may improve the diagnostic yield (30).

The present study had several limitations. First, it was a

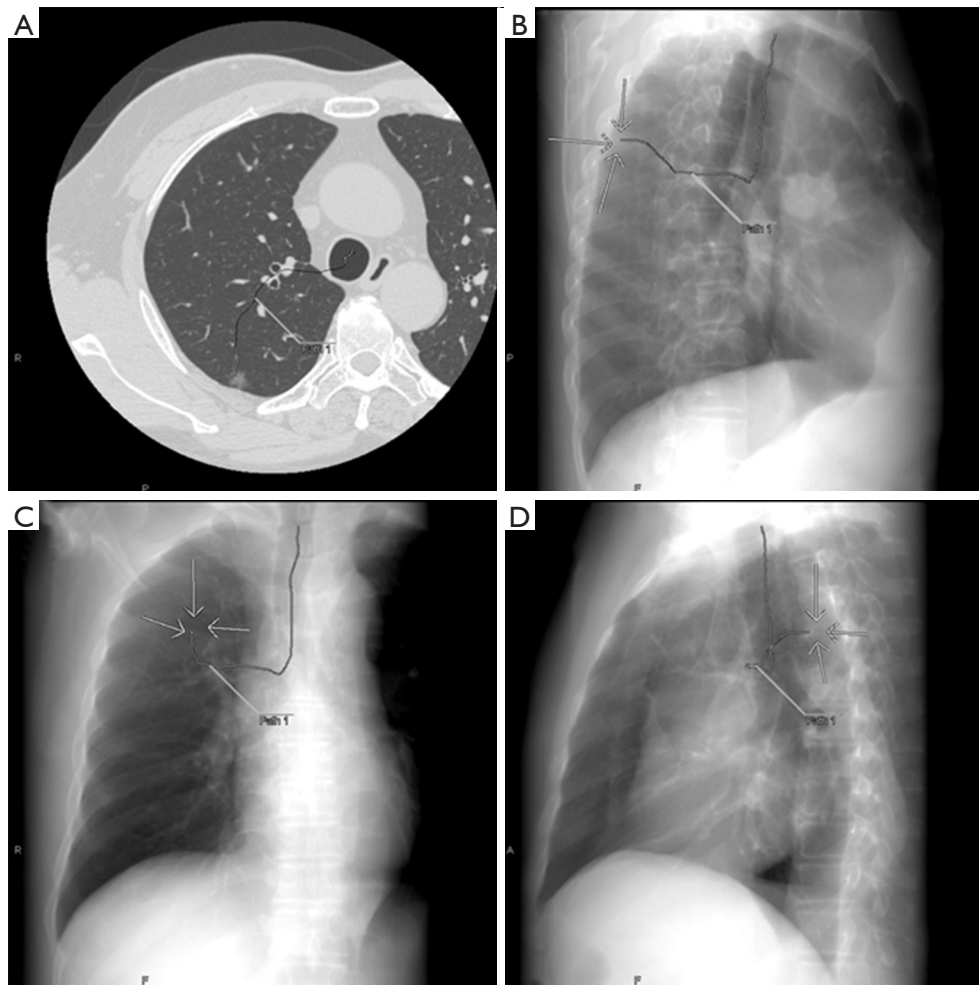


Figure 2 Virtual fluoroscopy (VF) shows the best working angle for the target lesion. Computed tomography shows a peripheral pulmonary lesion measuring 9.1 mm in the right S2 (A). VF shows that a right anterior oblique 60° angle (B) is the best working angle resulting in a long and wide trace line between the trachea and the target lesion (surrounded by arrows). At other angles, the target lesion is overlapped by a pulmonary artery and vertebrae (C,D), making the detection of the target lesion difficult and misleading the forceps.

retrospective, nonrandomized study conducted at a single center. Second, the type of bronchoscope and the number of sampling times varied with each procedure. Third, the fluoroscopy time during the procedure was not evaluated. The addition of VF findings to the conventional procedure might actually shorten the fluoroscopy time during the bronchoscopy. Finally, the influence of rapid on-site examinations during the procedures on the diagnostic yield was not evaluated.

Conclusions

The addition of VF to EBUS-GS and VB improved the

diagnostic yield of bronchoscopy for GGNs that were not visible on X-ray fluoroscopy images. Prospective, randomized studies are warranted for more accurate analysis.

Acknowledgements

We would like to thank Koji Tsuta and Noriko Motoi for supporting the pathologic examinations.

Footnote

Conflicts of Interest: The authors have no conflicts of interest to declare.

Ethical Statement: This study was approved by the National Cancer Center Institutional Review Board (No. 2012-278). Written informed consent was obtained from all the patients prior to bronchoscopy.

References

- Henschke CI, Yankelevitz DE, Mirtcheva R, et al. CT screening for lung cancer: frequency and significance of part-solid and nonsolid nodules. *AJR Am J Roentgenol* 2002;178:1053-7.
- National Lung Screening Trial Research Team, Church TR, Black WC, et al. Results of initial low-dose computed tomographic screening for lung cancer. *N Engl J Med* 2013;368:1980-91.
- Li F, Sone S, Abe H, et al. Malignant versus benign nodules at CT screening for lung cancer: comparison of thin-section CT findings. *Radiology* 2004;233:793-8.
- Lee HY, Lee KS. Ground-glass opacity nodules: histopathology, imaging evaluation, and clinical implications. *J Thorac Imaging* 2011;26:106-18.
- Wiener RS, Schwartz LM, Woloshin S, et al. Population-based risk for complications after transthoracic needle lung biopsy of a pulmonary nodule: an analysis of discharge records. *Ann Intern Med* 2011;155:137-44.
- Inoue D, Gobara H, Hiraki T, et al. CT fluoroscopy-guided cutting needle biopsy of focal pure ground-glass opacity lung lesions: diagnostic yield in 83 lesions. *Eur J Radiol* 2012;81:354-9.
- Smith MA, Battafarano RJ, Meyers BF, et al. Prevalence of benign disease in patients undergoing resection for suspected lung cancer. *Ann Thorac Surg* 2006;81:1824-8; discussion 1828-9.
- Grogan EL, Weinstein JJ, Deppen SA, et al. Thoracic operations for pulmonary nodules are frequently not futile in patients with benign disease. *J Thorac Oncol* 2011;6:1720-5.
- Flores R, Bauer T, Aye R, et al. Balancing curability and unnecessary surgery in the context of computed tomography screening for lung cancer. *J Thorac Cardiovasc Surg* 2014;147:1619-26.
- Tomiyama N, Yasuhara Y, Nakajima Y, et al. CT-guided needle biopsy of lung lesions: a survey of severe complication based on 9783 biopsies in Japan. *Eur J Radiol* 2006;59:60-4.
- Asano F, Aoe M, Ohsaki Y, et al. Bronchoscopic practice in Japan: a survey by the Japan Society for Respiratory Endoscopy in 2010. *Respirology* 2013;18:284-90.
- Izumo T, Sasada S, Chavez C, et al. The diagnostic utility of endobronchial ultrasonography with a guide sheath and tomosynthesis images for ground glass opacity pulmonary lesions. *J Thorac Dis* 2013;5:745-50.
- Ikezawa Y, Sukoh N, Shinagawa N, et al. Endobronchial ultrasonography with a guide sheath for pure or mixed ground-glass opacity lesions. *Respiration* 2014;88:137-43.
- Ikezawa Y, Shinagawa N, Sukoh N, et al. Usefulness of Endobronchial Ultrasonography With a Guide Sheath and Virtual Bronchoscopic Navigation for Ground-Glass Opacity Lesions. *Ann Thorac Surg* 2017;103:470-5.
- Minezawa T, Okamura T, Yatsuya H, et al. Bronchus sign on thin-section computed tomography is a powerful predictive factor for successful transbronchial biopsy using endobronchial ultrasound with a guide sheath for small peripheral lung lesions: a retrospective observational study. *BMC Med Imaging* 2015;15:21.
- Fukusumi M, Ichinose Y, Arimoto Y, et al. Bronchoscopy for Pulmonary Peripheral Lesions With Virtual Fluoroscopic Preprocedural Planning Combined With EBUS-GS: A Pilot Study. *J Bronchology Interv Pulmonol* 2016;23:92-7.
- Kim TJ, Lee JH, Lee CT, et al. Diagnostic accuracy of CT-guided core biopsy of ground-glass opacity pulmonary lesions. *AJR Am J Roentgenol* 2008;190:234-9.
- Kurimoto N, Miyazawa T, Okimasa S, et al. Endobronchial ultrasonography using a guide sheath increases the ability to diagnose peripheral pulmonary lesions endoscopically. *Chest* 2004;126:959-65.
- Yamada N, Yamazaki K, Kurimoto N, et al. Factors related to diagnostic yield of transbronchial biopsy using endobronchial ultrasonography with a guide sheath in small peripheral pulmonary lesions. *Chest* 2007;132:603-8.
- Sasada S, Izumo T, Chavez C, et al. Blizzard Sign as a specific endobronchial ultrasound image for ground glass opacity: A case report. *Respir Med Case Rep* 2014;12:19-21.
- Izumo T, Sasada S, Chavez C, et al. Radial endobronchial ultrasound images for ground-glass opacity pulmonary lesions. *Eur Respir J* 2015;45:1661-8.
- Izumo T, Sasada S, Chavez C, et al. The diagnostic value of histology and cytology samples during endobronchial ultrasound with a guide sheath. *Jpn J Clin Oncol* 2015;45:362-6.
- Matsumoto Y, Izumo T, Sasada S, et al. Diagnostic utility of endobronchial ultrasound with a guide sheath under the computed tomography workstation (ziostation) for small peripheral pulmonary lesions. *Clin Respir J* 2017;11:185-92.
- Naidich DP, Sussman R, Kutcher WL, et al. Solitary

- pulmonary nodules. CT-bronchoscopic correlation. *Chest* 1988;93:595-8.
25. Gaeta M, Pandolfo I, Volta S, et al. Bronchus sign on CT in peripheral carcinoma of the lung: value in predicting results of transbronchial biopsy. *AJR Am J Roentgenol* 1991;157:1181-5.
 26. Kanda Y. Investigation of the freely available easy-to-use software 'EZR' for medical statistics. *Bone Marrow Transplant* 2013;48:452-8.
 27. MacMahon H, Austin JH, Gamsu G, et al. Guidelines for management of small pulmonary nodules detected on CT scans: a statement from the Fleischner Society. *Radiology* 2005;237:395-400.
 28. Goo JM, Park CM, Lee HJ. Ground-glass nodules on chest CT as imaging biomarkers in the management of lung adenocarcinoma. *AJR Am J Roentgenol* 2011;196:533-43.
 29. Wang Memoli JS, Nietert PJ, Silvestri GA. Meta-analysis of guided bronchoscopy for the evaluation of the pulmonary nodule. *Chest* 2012;142:385-93.
 30. Takai M, Izumo T, Chavez C, et al. Transbronchial needle aspiration through a guide sheath with endobronchial ultrasonography (GS-TBNA) for peripheral pulmonary lesions. *Ann Thorac Cardiovasc Surg* 2014;20:19-25.

Cite this article as: Nakai T, Izumo T, Matsumoto Y, Tsuchida T. Virtual fluoroscopy during transbronchial biopsy for locating ground-glass nodules not visible on X-ray fluoroscopy. *J Thorac Dis* 2017;9(12):5493-5502. doi: 10.21037/jtd.2017.10.01